

Searching for three-nucleon short-range correlations

Misak M. Sargsian¹, Donal B. Day², Leonid L. Frankfurt³, and Mark I. Strikman⁴

¹ *Department of Physics, Florida International University, Miami, FL 33199, USA*

² *Department of Physics, University of Virginia, Charlottesville, VA 22904, USA*

³ *Sackler School of Exact Sciences, Tel Aviv University, Tel Aviv, 69978, Israel*

⁴ *Department of Physics, Pennsylvania State University, University Park, PA 16802*

(Dated: November 1, 2019)

Three nucleon short range correlations (SRCs) are one of the most elusive structures in nuclei. Their observation and the subsequent study of their internal makeup will have a significant impact on our understanding of the dynamics of super-dense nuclear matter which exists at the cores of neutron stars. We discuss the kinematic conditions and observables that are most favorable for probing 3N-SRCs in inclusive electro-nuclear processes and make a prediction for a quadratic dependence of the probabilities of finding a nucleon in 2N- and 3N- SRCs. We demonstrate that this prediction is consistent with the limited high energy experimental data available, suggesting that we have observed, for the first time, 3N-SRCs in electro-nuclear processes. Our analysis enables us to extract $a_3(A, Z)$, the probability of finding 3N-SRCs in nuclei relative to the $A=3$ system.

I. INTRODUCTION:

Three nucleon short-range correlations (3N-SRCs), in which three nucleons come close together, are unique arrangements in strong interaction physics. 3N SRC's have a single nucleon with very large momentum ($\gtrsim 700$ MeV/c) balanced by two nucleons of comparable momenta. Unlike two-nucleon short-range correlations (2N-SRCs), 3N-SRCs have never been probed directly through experiment. As the consequence of the factorization of short-distance effects from low momentum collective phenomena [1, 2], 2N- and 3N- SRCs dominate the high momentum component of nuclear wave function which is almost universal up to a scale factor (see e.g.[1, 3]).

The dynamics of three-nucleon short-range configurations reside at the borderline of our knowledge of nuclear forces making their exploration a testing ground for “beyond the standard nuclear physics” phenomena such as irreducible three-nucleon forces, inelastic transitions in 3N systems as well as the transition from hadronic to quark degrees of freedom. Their strength is expected to grow faster with the local nuclear density than the strength of 2N-SRCs [1, 2]. As a result, their contribution will be essential for an understanding of the dynamics of super-dense nuclear matter (see e.g. Ref. [4]).

Until recently a straightforward experimental probe of 2N- and 3N-SRCs was impossible due to the requirements of high-momentum transfer nuclear reactions being measured in very specific kinematics in which the expected cross sections are very small (see Ref.[1] and references therein). With the advent of the high energy (6 GeV) and high intensity continuous electron accelerator at Jefferson Lab (JLab) in the late 1990's, an unprecedented exploration of nuclear structure became possible, opening a new window to multi-nucleon SRCs.

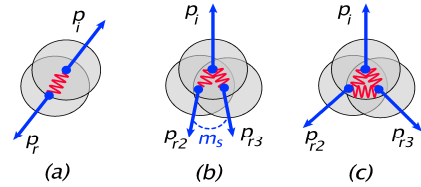


FIG. 1: (a) Geometry of 2N-SRCs, $\mathbf{p}_r \approx -\mathbf{p}_i$. Two configurations of 3N-SRCs: (b) Configuration in which recoil nucleon momenta $\mathbf{p}_{r2}, \mathbf{p}_{r3} \sim -\mathbf{p}_i/2$, (c) configuration in which $p_{r2} \sim p_{r3} \sim p_i$. Here m_s is the invariant mass of the recoiling 2N system.

II. TWO NUCLEON SHORT RANGE CORRELATIONS (2N-SRCs)

The first dedicated study of 2N-SRCs in inclusive, $A(e, e')X$, high momentum transfer reactions revealed a plateau in the ratios of per nucleon cross sections of heavy nuclei to the deuteron [5] measured at Stanford Linear Accelerator Center (SLAC) with momentum transfer, $Q^2 \gtrsim 2$ GeV² and Bjorken variable $x > 1.5$. Here $x = \frac{Q^2}{2m_N q_0}$ with m_N the nucleon mass and q_0 the transferred energy to the nucleus, and for a nucleus A , $0 < x < A$. The observed plateau, largely insensitive to Q^2 and x , sets the parameter $a_2(A, Z)$ [6] which is the probability of finding 2N-SRCs in the ground state of the nucleus A relative to the deuteron. These plateaus were confirmed in inclusive cross section ratios of nuclei A to ${}^3\text{He}$ [7, 8], at similar kinematics with the magnitude of plateaus taken to be related to the relative probability, $\frac{a_2(A, Z)}{a_2({}^3\text{He})}$. Qualitatively and quantitatively the latter results were in agreement with Ref.[5]. These, together with more recent and dedicated measurements of the nuclear to the deuteron inclusive cross section ratios[9], provided compelling evidence for the sizable ($\sim 20\%$) high momentum component of the ground state nuclear wave function for medium to heavy nuclei originating from 2N-SRCs.

While inclusive processes provided the first evidence

for 2N-SRCs and an estimate of their probabilities, $a_2(A, Z)$, the details of correlation dynamics have been obtained mainly from semi-inclusive experiments in which one or both nucleons from 2N-SRCs were detected. The first $A(p, ppn)X$ experiments at high momentum transfer were performed at Brookhaven National Laboratory[10, 11]. The theoretical analysis of these experiments gave the striking result that the probability of finding proton-neutron combinations in 2N-SRCs exceeds by almost a factor of 20 the probabilities for proton-proton and neutron-neutron SRCs[12]. This result was subsequently confirmed in semi-inclusive electroproduction reactions at JLab[13, 14] and both are understood as arising from the dominance of the tensor component in the NN interaction at distances $|r_1 - r_2| \lesssim 1$ fm [15, 16]. This reinforced the conclusion that the nucleons have been isolated in SRCs with separations much smaller than average inter-nucleon distances. The dominance of the pn component in 2N-SRCs suggested a new prediction for momentum sharing between high momentum protons and neutrons in asymmetric nuclei[17] where the minority component (say protons in neutron rich nuclei) will dominate the high momentum component of the nuclear wave function. This prediction was confirmed indirectly in $A(e, e'p)X$ and $A(e, e'pp)X$ experiments[18] and directly in $A(e, e'p)X$ and $A(e, e'n)X$ processes in which proton and neutron constituents of 2N-SRCs have been probed independently[19, 20]. The momentum sharing effects also arise from variational Monte-Carlo calculations for light asymmetric nuclei[21] as well as in model calculations of nuclear wave functions for medium to heavy nuclei[22].

In addition to measuring the isospin content of 2N-SRCs, several experimental analyses[11, 14, 23] established a detailed “geometrical” picture of 2N-SRCs consisting of two overlapping nucleons having relative momentum between 250 – 650 MeV/c with back-to-back angular correlations (Fig.1(a)) and with moderate center of mass momentum, $\lesssim 150$ MeV/c, for nuclei ranging from ${}^4\text{He}$ to ${}^{208}\text{Pb}$ [23]. Several recent reviews[2, 3, 24–26] have documented extensively the recent progress in the investigation of 2N-SRCs in a wide range of atomic nuclei.

III. THREE NUCLEON SHORT RANGE CORRELATIONS (3N-SRCs)

Despite an impressive progress achieved in studies of 2N-SRCs the confirmation of 3N-SRCs remains arguable. One signature of 3N-SRCs is the onset of the *plateau* in the ratio of inclusive cross sections of nuclei A and ${}^3\text{He}$ in the kinematic region of $x > 2$ similar to the plateau observed for 2N-SRCs in the region of $1.5 < x < 2$ and discussed above. The first observation of a plateau at $x > 2$ was claimed in Ref.[8]. However it was not confirmed by subsequent measurements[9, 27]. The source of this disagreement has been traced to the poor reso-

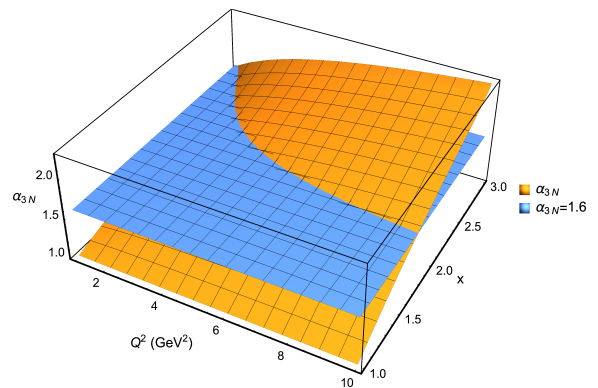


FIG. 2: Kinematics of 3N-SRCs. The surface above the horizontal plane at $\alpha_{3N} = 1.6$ defines the kinematics most optimal for identification of 3N-SRCs in inclusive processes. In this calculation we assumed a minimal mass for $m_S = 2m_N$ which corresponds to the maximal contribution to the nuclear spectral function with $k_\perp = 0$ and $\beta = 1$ (see Eq.(1)).

lution at $x > 2$ of the experiment of Ref.[8] which led to bin migration[28] where events move from smaller to higher x . Additionally, as it will be shown below, the absence of a plateau is related to the the modest invariant momentum transfer, Q^2 covered in Ref. [8].

To quantify the last statement we first need to identify the dominant structure of 3N-SRCs in the nuclear ground state. The problem is that while for 2N-SRCs the correlation geometry is straightforward (two fast nucleons nearly balancing each other, Fig.1(a)), in the case of 3N-SRCs the geometry of balancing three fast nucleons is not unique - ranging from configurations in which two almost parallel spectator nucleons with momenta, $\sim -\frac{\mathbf{p}_i}{2}$ balance the third nucleon with momentum \mathbf{p}_i , Fig.1(b)), to the configurations in which all three nucleons have momenta p_i with relative angles $\approx 120^\circ$ Fig.1(c)). The analysis of 3N systems in Ref.[15] demonstrated that configurations in which two recoil nucleons have the smallest possible mass, $m_S \sim 2m_N$, dominate the 3N-SRC nuclear spectral function at lower excitation energy. This allows us to conclude [29] that in inclusive scattering, which integrates over the nuclear excitation energies, the dominant contribution to 3N-SRCs originates from arrangements similar to Fig.1(b)) with $m_S \gtrsim 2m_N$.

With the dominant mechanism of 3N-SRCs identified we are able to develop the kinematic requirements to expose 3N correlations in inclusive eA scattering. We use the fact that, due to relativistic nature of SRC configurations, the most natural description is achieved through the light-cone (LC) nuclear spectral functions[6, 30] in which the correlated nucleons are described by their nuclear light-cone momentum fractions, α_i and transverse momentum $p_{i,\perp}$. In inclusive scattering one probes the spectral function integrated over the LC momenta of the correlated recoil nucleons, residual nuclear excitation energy and the transverse momentum of the interacting nucleon. This corresponds to the LC density matrix of the

nucleus $\rho_A(\alpha_N)$, where α_N is the LC momentum fraction of the nucleus carried by the interacting nucleon. It can be shown[31] that $\rho_A(\alpha_N)/\alpha$ is analogous to the partonic distribution function in QCD, $f_i(x)$ where x describes the LC momentum fraction of the nucleon carried by the interacting quark.

To evaluate the LC momentum fraction, α_N (henceforth α_{3N}) describing the interacting nucleon in the 3N-SRC, we consider the kinematic condition of quasielastic scattering from a 3N system: $q + 3m_N = p_f + p_S$, where q , p_f and p_S are the four momenta of the virtual photon, final struck nucleon and recoil two-nucleon system respectively. One defines the LC momentum fraction of the interacting nucleon, $\alpha_{3N} = 3 - \alpha_S$, where $\alpha_S \equiv 3 \frac{E_S - p_S^z}{E_{3N} - p_{3N}^z}$ is the light-cone fraction of the two spectator nucleons in the center of mass of the $\gamma^*(3N)$ system with $z||q$. Using the boost invariance of the light-cone momentum fractions one arrives at the following lab-frame expression (see Ref.[29] for details) :

$$\alpha_{3N} = 3 - \frac{q_- + 3m_N}{2m_N} \left[1 + \frac{m_S^2 - m_N^2}{W_{3N}^2} + \sqrt{\left(1 - \frac{(m_S + m_N)^2}{W_{3N}^2}\right) \left(1 - \frac{(m_S - m_N)^2}{W_{3N}^2}\right)} \right], \quad (1)$$

where $W_{3N}^2 = (q + 3m_N)^2 = Q^2 \frac{3-x}{x} + 9m_N^2$ and $q_- = q_0 - q$ with q_0 and q being energy and momentum transfer in the lab with $z||\mathbf{q}$. The invariant mass of the spectator 2N system, $m_S^2 = 4 \frac{m_N^2 + k_\perp^2}{\beta(2-\beta)}$ where \mathbf{k}_\perp is the transverse component of the relative momentum of the 2N system with respect to \mathbf{p}_S and β is the light-front momentum fraction of p_S carried by the spectator nucleon ($0 \leq \beta \leq 2$). Inclusive reactions integrate over the nuclear spectral function and k_\perp and m_s are not determined experimentally.

The expression for α_{3N} , Eq. (1), makes it possible to identify the kinematical conditions most appropriate for the isolation of 3N-SRCs in inclusive $A(e, e')X$ reactions. This is done by identifying the minimal value of α_{3N} above which one expects the contribution of 3N-SRCs to dominate. First, the threshold can be established from our experience of studying 2N-SRCs. In this case we know that 2N-SRCs in inclusive processes dominate at $\alpha_N \geq 1.3$ which corresponds to an internal longitudinal momenta of $\sim 300 - 350$ MeV/c. Hence for 3N-SRCs one needs at least $p_{min} \gtrsim 700$ MeV/c, corresponding to $\alpha_{3N} \gtrsim 1.6$, which will allow two high momentum spectator nucleons to belong to a 3N-SRCs. This minimal value for α_{3N} is validated by the studies of the fast backward nucleon production in pA scattering within the few-nucleon correlation model [6] which indicate that the transition from 2N- to 3N- SRCs occurs at $\alpha \sim 1.6 - 1.7$.

As α_{3N} increases above 1.6 the contribution of 2N-SRCs is suppressed relative to 3N-SRCs. This is because as the LC momentum fraction grows, the relative momentum in the 2N system grows much faster than the same quantity in the 3N system. Thus, in the further

discussions we will set $\alpha_{3N} = 1.6$ as the threshold value, above which one expects the 3N-SRCs to dominate in inclusive scattering. This minimal value for α_{3N} allows us to identify the kinematic parameters most promising for probing 3N-SRCs as illustrated in Fig. 2. The figure shows the relevant kinematics corresponding to the α_{3N} surface being above the $\alpha_{3N} = 1.6$ plane. This identifies the Q^2 and x domains favorable for probing 3N-SRCs. In particular, one observes that starting around $Q^2 \gtrsim 2.5 - 3$ GeV² one gains enough kinematical range in the $x > 2$ domain that one expects to observe 3N-SRCs.

Another advantage of considering 3N-SRCs in terms of α_{3N} , is that at sufficiently large Q^2 the LC momentum distribution function $\rho_A(\alpha_{3N})$ is not altered by final state hadronic interactions (FSIs). The important feature in the high energy limit is that FSIs redistribute the p_\perp strength in the nuclear spectral function leaving $\rho_A(\alpha_{3N})$ practically unchanged[32–34]. In this limit the distortion of α_{3N} due to FSI can be evaluated as[32]:

$$\delta\alpha \approx \frac{x^2}{Q^2} \frac{2m_N E_R}{\left(1 + \frac{4m_N^2 x^2}{Q^2}\right)}, \quad (2)$$

where E_R is the kinetic energy of the recoil two nucleon system. The estimates made in Ref.[29] indicate that for $Q^2 \sim 3$ GeV² FSI may alter α_{3N} by not more than 8% which is too small to shift the mean field nucleon, $\alpha_N \approx 1$, to the 3N-SRC domain at $\alpha_{3N} \geq 1.6$.

IV. SIGNATURES OF 3N-SRCs

The cross section in inclusive electron scattering at high Q^2 is factorized in the form[6]:

$$\sigma_{eA} \approx \sum_N \sigma_{eN} \rho_A^N(\alpha_N), \quad (3)$$

where σ_{eN} is the elastic electron-bound nucleon scattering cross section and $\rho_A^N(\alpha_N)$ is the light-front density matrix of the nucleus at a given LC momentum fraction, α_N of the probed nucleon. This is analogous to the QCD factorization in inclusive deep-inelastic scattering off the nucleon, in which the cross section is a product of a hard electron-parton scattering cross section and partonic distribution function.

The local property of SRCs suggests that $\rho_A(\alpha_N)$ in the correlation region to be proportional to the light-front density matrix of the two- and three-nucleon systems[5, 6]. This expectation leads to the prediction of the plateau for the ratios of inclusive cross sections in the SRC region that has been confirmed for 2N-SRCs. Similar to 2N-SRCs for the 3N-SRC one predicts a plateau for the experimental cross section ratios such as:

$$R_3(A, Z) = \frac{3\sigma_A(x, Q^2)}{A\sigma_{3He}(x, Q^2)} \Big|_{\alpha_{3N} > \alpha_{3N}^0}, \quad (4)$$

where α_{3N}^0 is the threshold value for the α_{3N} above which one expects onset of 3N-SRCs (taken as ~ 1.6 as described above). To quantify the strength of 3N-SRCs we introduce a parameter $a_3(A, Z)$ [29]:

$$a_3(A, Z) = \frac{3}{A} \frac{\sigma_{eA}}{(\sigma_{e^3He} + \sigma_{e^3H})/2}, \quad (5)$$

representing an intrinsic nuclear property related to the probability of finding 3N-SRCs in the nuclear ground state. If a plateau is observed in the 3N-SRC region of α_{3N} then the ratio $R_3(A, Z)$ in Eq.(4) can be used to extract $a_3(A, Z)$ as follows[29]:

$$a_3(A, Z) = R_3(A, Z) \frac{(2\sigma_{ep} + \sigma_{en})/3}{(\sigma_{ep} + \sigma_{en})/2}. \quad (6)$$

The status of the experimental observation of the scaling in the ratio of Eq.(4) is as follows: The E02-109 experiment[38] provided a high accuracy ratios, in the 2N-SRC region, at large momentum transfer for a wide range of nuclei[9]. This experiment covered some part of the 3N-SRC kinematic region with lesser quality of data (see also Refs.[37–40]), providing an indication of a plateau in the cross section ratios beginning at $x > 2$ once Q^2 is sufficiently high.

In Ref.[29] it was pointed out that the above-mentioned data [9, 37, 38] suffered from a collapse of the 3He cross section between $x = 2.68$ and $x = 2.85$ due to difficulties with the subtraction of the Aluminum target walls. This issue arose from the relatively small diameter of the target cell (4 cm) combined with the fact that $\sigma^{Al} \gg \sigma^{^3He}$ at large x as $\sigma^{^3He}$ must go to 0 at its kinematic limit, $x = 3$. The cross section ratio in Ref. [9] was made possible by the following: First the inverted ratio $^3He/{}^4He$ was formed and then rebinned - combining three bins into one for $x \geq 1.15$. Subsequently the bins in the inverted ratio that had error bars falling below zero were moved along a truncated gaussian, such that the lower edge of the error bar was at zero. The ratio was then inverted to give the ratio for ${}^4He/{}^3He$ shown in Figure 3 of Ref. [9] and as the triangles in Fig. 3 below. The use of a truncated gaussian gave rise to the asymmetric error bars seen in the ratios.

As an alternative to the somewhat unconventional procedure above, we have used the following approach to substitute the 3He data of Refs.[9, 37, 38] in 3N-SRC region: We have replaced the problematic data between $x = 2.68$ and $x = 2.85$ ($1.6 \leq \alpha_{3N} \leq 1.8$), point by point, by employing a y -scaling function $F(y)$ [41–43] fit to the SLAC data [35, 36] measured at a comparable Q^2 . A simple, two parameter fit $F(y) = a \exp(-by)$, limited to the range $1.6(y = -0.7) \leq \alpha_{3N} \leq 1.8(y = -1.1)$ provides a good description of the the SLAC data[29]. We preserved the absolute error of the E02019 data set [9, 37, 38] rather than the smaller errors from the fit. The fit parameters are $a = 0.296$ and $b = 8.241$.

Note that the above approach was first used in Ref. [5], which provided the first evidence of 2N-SRCs through

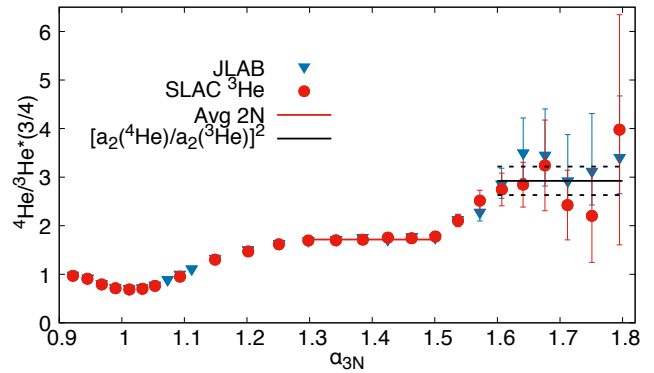


FIG. 3: The α_{3N} dependence of the inclusive cross section ratios for 4He to 3He , triangles - JLAB data [9, 37], circles - ratios when using a parameterization of SLAC 3He cross sections [35, 36]. The horizontal line at $1.3 \leq \alpha_{3N} < 1.5$ identifies the magnitude of the 2N-SRC plateau. The line for $\alpha_{3N} > 1.6$ is Eq.(10) with a 10% error introduced to account for the systematic uncertainty in $a_2(A, Z)$ parameters across all measurements. The data correspond to $Q^2 \approx 2.5 \text{ GeV}^2$ at $x = 1, \alpha_{3N} = 1$.

cross section ratios in inclusive scattering. The 2N-SRC results obtained have been confirmed by subsequent precision studies[7–9] in which the ratios were measured in single experiment.

It is also worth mentioning that in the case of 2N-SRC the adopted approach was more complicated than the one we employed in the current work. In Ref. [5] the data were combined to form the cross section ratios of nuclei (${}^3He, {}^4He, C, Al, Fe$ and Au) to the deuteron, covering a range in Q^2 from 0.9 to 3.2 (GeV/c)^2 . In the current analysis of 3N-SRCs, we worked at a single value of $Q^2 \approx 2.7 \text{ (GeV/c)}^2$ and, incidentally, the 3He data used in 1993 is the same set we employ here. The resulting ratios are displayed as red circles in Fig. 3.

Fig. 3 presents the results for the cross section ratios obtained within the two above described approaches. While both give similar results we consider the replacement of the data points between $x = 2.68$ and $x = 2.85$ ($1.6 \leq \alpha_{3N} \leq 1.8$) as a best alternative to the procedure adopted in Ref [9] in part because it allows a consistent treatment of the ratios for all A .

In Fig. 3 the plateau due to 2N-SRCs is clearly visible for $1.3 \leq \alpha_{3N} \leq 1.5$. In this region $\alpha_{3N} \approx \alpha_{2N}$ [29], where α_{2N} is the LC momentum fraction of the nucleon in the 2N-SRC. Because of this, we refer to the magnitude of this plateau as:

$$R_2(A, Z) = \frac{3\sigma_A(x, Q^2)}{A\sigma_{^3He}(x, Q^2)} \Big|_{1.3 \leq \alpha_{3N} \leq 1.5} = \frac{a_2(A)}{a_2(^3He)}. \quad (7)$$

The horizontal line in the region of $1.3 \leq \alpha_{3N} \leq 1.5$ is given by the right hand side of Eq. (7), in which the values of $a_2(^3He)$ and $a_2(A)$ are taken from the last column of

Table II in Ref. [44], an average of the SLAC, JLAB Hall C and JLAB Hall B results. The magnitude of the horizontal solid line in the region of $1.6 \leq \alpha_{3N} \leq 1.8$, is the prediction of $R_{3N}(A, Z) \approx R_{2N}^2(A, Z)$ which will be explained in the next section. We assigned a 10% error to this prediction (dashed lines) related to the uncertainty of $a_2(A, Z)$ magnitudes across different measurements.

As Fig.3 shows the data at $\alpha_{3N} > 1.6$ are consistent with the prediction of the onset of the new plateau in the 3N-SRC region and that its magnitude is proportional to R_{2N}^2 .

With a set of ^3He data obtained in the above discussed approach we are able to estimate the ratios for other nuclei, including, ^9Be , ^{12}C , ^{64}Cu , and ^{197}Au , albeit with larger uncertainties[29].

The large experimental uncertainties in evaluation of the ratios for ^4He (Fig.3) and for heavier nuclei[29] do not allow us to claim unambiguously the onset of the plateau at $\alpha_{3N} \geq 1.6$. However one can evaluate the validity of such a plateau by comparing one- and two- parameter fits to the experimental ratios in the $\alpha_{3N} \geq 1.6$ region. The one-parameter fit in the 3N-region gives the values (R_3^{exp}) of the plateaus as seen in Figure 4(a) along with our prediction of Eq. (10). R_3^{exp} is also listed in Table I. A two-parameter linear fit, returns errors on the parameters nearly as large as the parameters themselves and a correlation matrix indicating that the second parameter is redundant, providing no additional information.

V. 3N-SRCS AND THE pn DOMINANCE:

In Fig.1(b) the 3N-SRC is produced in the sequence of two short-range NN interactions in which the nucleon with the largest momentum interacts with the external probe[29, 30]. The presence of short-range NN interactions in 3N-SRC configurations tells us that the recently observed pn -SRC dominance[12–14] is critical to our understanding of 3N-SRCS.

For 3N-SRCS one expects that only pnp or npn configurations to contribute, with the pn short-range interaction playing role of a “catalyst” in forming a fast interacting nucleon with momentum, p_i (Fig.1(b)). For example, in the case of pnp configuration, the neutron will play the role of intermediary in furnishing a large momentum transfer to one of the protons with two successive short range pn interactions. Quantitatively such a scenario is reflected in the nuclear light-front density matrix in the 3N-SRC domain, $\rho_{A(3N)}^N(\alpha_N)$, being expressed through the convolution of two pn -SRC density matrixes, $\rho_{A(pn)}^N(\alpha, p_\perp)$ as follows:

$$\rho_{A(3N)}^N(\alpha_N, p_\perp) \approx \sum_{i,j} \int F(\alpha'_i, p_{i\perp}, \alpha'_j, p_{j\perp}) \times \rho_{A(pn)}^N(\alpha'_i, p'_{i\perp}) \rho_{A(pn)}^N(\alpha'_j, p'_{j\perp}) d\alpha_i d^2 p_{j\perp} d\alpha_i d^2 p_{j\perp}, \quad (8)$$

where $(\alpha'_{i/j}, p'_{i/j\perp})$, are the LC momentum fractions and transverse momenta of spectator nucleons in the center of

mass of the pn SRCS. According to the pn dominance[17]:

$$\rho_{A(pn)}^N(\alpha, p_\perp) \approx \frac{a_2(A, Z)}{2X_N} \rho_d(\alpha, p_\perp), \quad (9)$$

where $X_N = Z/A$ or $(A - Z)/A$ is the relative fraction of the proton or neutron in the nucleus and $\rho_d(\alpha, p_\perp)$ is the light-front density function of the deuteron at $\alpha \geq 1.3$. The factor $F(\alpha'_i, p_{i\perp}, \alpha'_j, p_{j\perp})$ is a smooth function of LC momenta and accounts for the phase factors of nucleons in the intermediate state between the sequential pn interactions with $0 < \alpha'_{i/j} < 2$.

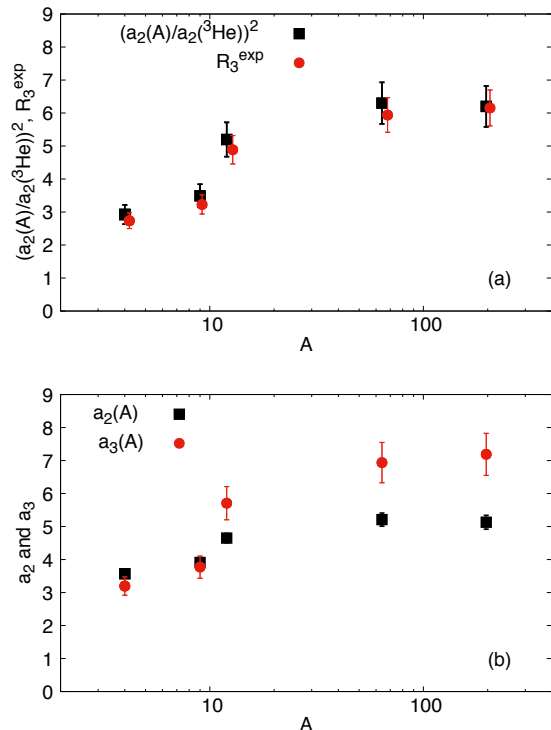


FIG. 4: (a) The A dependence of the experimental evaluation of R_3 compared with the prediction of Eq.10. (b) The A dependence of $a_3(A, Z)$ parameter compared to $a_2(A, Z)$ of Ref.[9].

It follows, from Eq.(8) and the expression of $\rho_{A(pn)}^N(\alpha, p_\perp)$ in Eq.(9), that the strength of 3N-SRCS is $\propto a_2^2(A, Z)$. This is evident by calculating R_3 in Eq.(4) using the relation (3) and the conjecture of Eq.(8), which leads to[29]:

$$R_3(A, Z) = \frac{9}{8} \frac{(\sigma_{ep} + \sigma_{en})/2}{(2\sigma_{ep} + \sigma_{en})/3} R_2^2(A, Z) \approx \left(\frac{a_2(A, Z)}{a_2(^3\text{He})} \right)^2, \quad (10)$$

where $\sigma_{ep} \approx 3\sigma_{en}$ in the considered $Q^2 \sim 3 \text{ GeV}^2$ range. As Fig.3 shows the prediction of $R_3 \approx R_2^2$ is in agreement with the experimental per nucleon cross section ratios of ^4He to ^3He targets. There is a similar agreement for other nuclei including ^9Be , ^{12}C , ^{64}Cu and ^{197}Au [29].

To test the prediction of Eq.(10) quantitatively we evaluated the weighted average of $R_3^{exp}(A, Z)$ for $\alpha_{3N} >$

TABLE I: Numerical values a_2 [44], R_2 (Eq. 7), R_3^{exp} (the weighted average in the 3N region) and a_3 (Eq. 6)).

A	a_2	R_2	R_3^{exp}	a_3
3	2.13 ± 0.04	1	NA	NA
4	3.57 ± 0.09	1.68 ± 0.03	2.74 ± 0.24	3.20 ± 0.28
9	3.91 ± 0.12	1.84 ± 0.04	3.23 ± 0.29	3.77 ± 0.34
12	4.65 ± 0.14	2.18 ± 0.04	4.89 ± 0.43	$5.71 \pm 0, 50$
64	5.21 ± 0.20	2.45 ± 0.04	5.94 ± 0.52	6.94 ± 0.77
197	5.13 ± 0.21	2.41 ± 0.05	6.15 ± 0.55	7.18 ± 0.64

1.6 and compared them with the magnitude of $(\frac{a_2(A,Z)}{a_2(3He)})^2$ in which $a_2(A, Z)$'s are taken from Ref. [44]. The results in which the ^3He cross section was taken from the $F(y)$ fit to the SLAC data are presented in Fig.4(a) and in Table I. They show good agreement with the prediction of Eq.(10) for the full range of nuclei. We investigated the sensitivity of the weighted average of $R_3(A, Z)$ on the lower limit of α_{3N} (before rebinning) and found that the results shown in Fig. 4(a) remain unchanged within errors which grow with a larger $\alpha_{3N} > 1.6$ cut.

The agreement presented in Fig.4(a) represents the strongest evidence yet for the presence of 3N-SRCs. If it is truly due to the onset of 3N-SRCs then one can use the measured R_3^{exp} ratios and Eq.(6) to extract the $a_3(A, Z)$ parameters characterizing the 3N - SRC probabilities in the nuclear ground state. The estimates of $a_3(A, Z)$ and comparisons with $a_2(A, Z)$ are given in Fig.4(b) (see also Table I). These comparisons show a faster rise for $a_3(A, Z)$ with A , consistent with the expectation of the increased sensitivity of 3N-SRCs to the local nuclear density[2]. If this result is verified in the future with better quality data and a wider range of nuclei then the evaluation of the parameter $a_3(A, Z)$ as a function of nuclear density and proton/neutron asymmetry together with $a_2(A, Z)$ can provide an important theo-

retical input for the exploration of the dynamics of super dense nuclear matter (see e.g. [45]).

VI. SUMMARY

Based on the theoretical analysis of a three-nucleon system we have concluded that the dominating mechanism of 3N-SRCs in inclusive processes corresponds to the situation in which the recoil mass of the 2N spectator system is close to a minimum. From that basis we derived a kinematic condition for the onset of 3N-SRCs in inclusive eA scattering which should result in the observation of a plateau in the ratio of cross sections of heavy to light nuclei, such as, $\frac{3}{A} \frac{\sigma^A}{\sigma^{3He}}$. The best quality data, available for large enough Q^2 (Fig.3), indicate a possible onset of such a plateau at $\alpha_{3N} > 1.6$. This first signature of 3N-SRCs is reinforced by the good agreement with the prediction of the quadratic ($R_3 \approx R_2^2$) dependence between the cross section ratios in the 3N-SRCs domain, R_3 , and the same ratio measured in the 2N-SRC region, R_2 . This agreement has allowed us, for the first time, to extract the parameter $a_3(A, Z)$ characterizing the strength of 3N-SRCs in the ground state wave function of the nucleus. Further measurements at larger Q^2 are necessary to confirm the observation made in this analysis. Precision data at large Q^2 in the 3N-SRC region can be secured in the forthcoming 12 GeV experiment at Jefferson Lab, E12-06-105[46].

Acknowledgments

This work is supported by the US Department of Energy grants: DE-FG02-96ER40950 (DBD), DE-FG02-01ER41172 (MSS) and DE-FG02-93ER40771 (MIS).

-
- [1] L. L. Frankfurt and M. I. Strikman, Phys. Rept. **76**, 215 (1981).
[2] L. Frankfurt, M. Sargsian and M. Strikman, Int. J. Mod. Phys. A **23**, 2991 (2008).
[3] C. Ciofi degli Atti, Phys. Rept. **590**, 1 (2015).
[4] H. Heiselberg and V. Pandharipande, Ann. Rev. Nucl. Part. Sci. **50**, 481 (2000).
[5] L. L. Frankfurt, M. I. Strikman, D. B. Day and M. Sargsian, Phys. Rev. C **48**, 2451 (1993).
[6] L. L. Frankfurt and M. I. Strikman, Phys. Rept. **160**, 235 (1988).
[7] K. S. Egiyan *et al.* [CLAS Collaboration], Phys. Rev. C **68**, 014313 (2003).
[8] K. S. Egiyan *et al.* [CLAS Collaboration], Phys. Rev. Lett. **96**, 082501 (2006).
[9] N. Fomin, *et al.*, Phys. Rev. Lett. **108**, 092502 (2012).
[10] J. L. S. Aclander *et al.*, Phys. Lett. B **453**, 211 (1999).
[11] A. Tang *et al.*, Phys. Rev. Lett. **90**, 042301 (2003)
[12] E. Piasetzky, M. Sargsian, L. Frankfurt, M. Strikman and J. W. Watson, Phys. Rev. Lett. **97**, 162504 (2006).
[13] R. Shneor *et al.* [Jefferson Lab Hall A Collaboration], Phys. Rev. Lett. **99**, 072501 (2007).
[14] R. Subedi, *et al.*, Science **320**, 1476 (2008).
[15] M. M. Sargsian, T. V. Abrahamyan, M. I. Strikman and L. L. Frankfurt, Phys. Rev. C **71**, 044615 (2005).
[16] R. Schiavilla, R. B. Wiringa, S. C. Pieper and J. Carlson, Phys. Rev. Lett. **98**, 132501 (2007).
[17] M. M. Sargsian, Phys. Rev. C **89**, no. 3, 034305 (2014).
[18] O. Hen, *et al.*, Science **346**, 614 (2014).
[19] M. Duer, *et al.* [CLAS Collaboration], Nature **560**, no. 7720, 617 (2018).
[20] M. Duer *et al.* [CLAS Collaboration], arXiv:1810.05343 [nucl-ex].
[21] R. B. Wiringa, R. Schiavilla, S. C. Pieper and J. Carlson, Phys. Rev. C **89**, no. 2, 024305 (2014).
[22] J. Ryckebusch, W. Cosyn and M. Vanhalst, J. Phys. G

- 42**, no. 5, 055104 (2015).
- [23] E. O. Cohen *et al.* [CLAS Collaboration], Phys. Rev. Lett. **121**, no. 9, 092501 (2018).
- [24] J. Arrington, D. W. Higinbotham, G. Rosner and M. Sargsian, Prog. Part. Nucl. Phys. **67**, 898 (2012).
- [25] N. Fomin, D. Higinbotham, M. Sargsian and P. Solvignon, Ann. Rev. Nucl. Part. Sci. **67**, 129 (2017).
- [26] O. Hen, G. A. Miller, E. Piasezky and L. B. Weinstein, Rev. Mod. Phys. **89**, no. 4, 045002 (2017).
- [27] Z. Ye *et al.* [Hall A Collaboration], Phys. Rev. C **97**, no. 6, 065204 (2018).
- [28] D. W. Higinbotham and O. Hen, Phys. Rev. Lett. **114**, no. 16, 169201 (2015).
- [29] D. B. Day, L. L. Frankfurt, M. M. Sargsian and M. I. Strikman, arXiv:1803.07629 [nucl-th].
- [30] O. Artilles and M. M. Sargsian, Phys. Rev. C **94**, no. 6, 064318 (2016).
- [31] A. J. Freese, M. M. Sargsian and M. I. Strikman, Eur. Phys. J. C **75**, no. 11, 534 (2015).
- [32] M. M. Sargsian, Int. J. Mod. Phys. E **10**, 405 (2001).
- [33] L. L. Frankfurt, M. M. Sargsian and M. I. Strikman, Phys. Rev. C **56**, 1124 (1997).
- [34] W. Boeglin and M. Sargsian, Int. J. Mod. Phys. E **24**, no. 03, 1530003 (2015).
- [35] D. Day *et al.*, Phys. Rev. Lett. **43**, 1143 (1979).
- [36] S. Rock *et al.*, Phys. Rev. C **26**, 1592 (1982).
- [37] N. Fomin *et al.*, Phys. Rev. Lett. **105**, 212502 (2010).
- [38] Jefferson Lab Experiment No. E-02-019, unpublished, 2002. https://www.jlab.org/exp_prog/proposals/02/PR02-019.pdf.
- [39] N. Fomin, PhD thesis, University of Virginia, 2007, arXiv:0812.2144.
- [40] N. Fomin, AIP Conf. Proc. **947**, 174 (2007).
- [41] D. B. Day *et al.*, Phys. Rev. Lett. **59**, 427 (1987).
- [42] I. Sick, D. Day and J. S. McCarthy, Phys. Rev. Lett. **45**, 871 (1980).
- [43] D. B. Day, J. S. McCarthy, T. W. Donnelly and I. Sick, Ann. Rev. Nucl. Part. Sci. **40**, 357 (1990).
- [44] J. Arrington, A. Daniel, D. Day, N. Fomin, D. Gaskell, and P. Solvignon, Phys. Rev. C **86**, 065204 (2012).
- [45] D. Ding, A. Rios, H. Dussan, W. H. Dickhoff, S. J. Witte, A. Polls, A. Carbone, Phys. Rev. C **94**, 025802 (2016).
- [46] Inclusive scattering from nuclei at $x > 1$ in the quasielastic and deeply inelastic regimes. https://www.jlab.org/exp_prog/proposals/06/PR12-06-105.pdf Jefferson Lab Experiment No. E12-06-105, unpublished, 2006.